

New Insights into the Synthesis, Morphology, and Growth of Periodic Mesoporous Organosilicas

Abdelhamid Sayari,^{*,†} Safia Hamoudi,[†] Yong Yang,[†] Igor L. Moudrakovski,[‡] and John R. Ripmeester[‡]

Department of Chemical Engineering and CERPIC, Université Laval, Ste-Foy, Quebec, Canada G1K 7P4, and Steacie Institute for Molecular Sciences, National Research Council, Ottawa, Ontario, Canada K1A 0R6

Received June 12, 2000. Revised Manuscript Received October 4, 2000

Periodic mesoporous organosilicas with two-dimensional and three-dimensional hexagonal as well as cubic ($Pm\bar{3}n$) symmetry were synthesized using bridged silsesquioxane species $(RO)_3Si-CH_2-CH_2-Si(RO)_3$ as precursors and cetyl- or octadecyltrimethylammonium chloride ($C_{16}TMACl$ or $C_{18}TMACl$) as structure-directing species. These materials were characterized by N_2 adsorption, SEM, TEM, and solid-state MAS NMR spectroscopy. ^{13}C and ^{29}Si NMR data showed unambiguously that all carbon atoms were covalently linked to Si. The cubic material obtained in the presence of $C_{16}TMACl$ and 1,2-bis(trimethoxysilyl)ethane (BTME) first formed into truncated rhombic dodecahedral particles that grew into spheres. The sample prepared in the presence of $C_{18}TMACl$ and BTME at 100 °C was entirely comprised of concentrically self-assembled 10- μm hexagonal rods. Using $C_{16}TMACl$ in the presence of 1,2-bis(triethoxysilyl)ethane (BTEE) at 95 °C afforded high-quality two-dimensional hexagonal organosilica comprised of unusually long (30–40 μm) faceted empty tubules.

Introduction

Since the discovery of the so-called M41S silicas,¹ the preparation of periodic mesoporous materials with different compositions has been among the strongest research themes in this field. The early work dealt with decorating the silica framework with various cations such as Al^{3+} , B^{3+} , Ti^{4+} , V^{5+} , and others with the purpose of preparing acid or selective oxidation catalysts.^{2–4} Subsequent work extended the compositional range of mesoporous materials to non-silica oxides^{5–7} and mixed oxides such as aluminos and vanadophosphates,^{6,7} sulfides,^{8–10} and metals.¹¹ Another strategy that attracted much attention was surface modification either through direct synthesis using organosilanes $(RO)_3SiR'$ or by postsynthesis grafting of metallic cations and other more sophisticated species.^{12,13}

However, it is only recently that bridged silsesquioxane species $(RO)_3Si-R'-Si(OR)_3$ were used to prepare periodic mesoporous organosilicas, leading to a new class of materials where the organic component is built in the walls of the channels^{14–18} instead of protruding into them. A number of bridged silsesquioxanes have already been successfully used as precursors. These included bis-silylated methylene, ethane, ethylene, acetylene, benzene, thiophene, bithiophene, and ferrocene. This new development is the result of combining the self-assembly approach for making ordered mesoporous materials, and the use of bridged silsesquioxanes, which have been known as precursors in sol–gel chemistry for some time.^{19,20} The purpose of the current paper was to further study the synthesis and growth of organosilicas using $(RO)_3Si-CH_2-CH_2-Si(OR)_3$ with $R = CH_3$ or C_2H_5 .

Experimental Section

Synthesis. Inspection of the first three papers^{14–16} devoted to periodic mesoporous organosilica showed that the materials

* To whom correspondence should be addressed: E-mail: sayari@gch.ulaval.ca. Phone: (418)656 3563. Fax: (418)656 5993.

[†] Université Laval.

[‡] National Research Council.

(1) Kresge, C. T.; Leonowicz, M. E.; Roth, W. J.; Vartuli, J. C.; Beck, J. S. *Nature* **1992**, *359*, 710.

(2) Sayari, A. *Chem. Mater.* **1996**, *8*, 1840.

(3) Sayari, A. *Stud. Surf. Sci. Catal.* **1996**, *102*, 1.

(4) Ying, J. Y.; Mehnert, C. P.; Wong, M. S. *Angew. Chem., Int. Ed.* **1999**, *38*, 57.

(5) Yang, P.; Zhao, D.; Margolese, D. I.; Chmelka, B. F.; Stucky, G. D. *Nature* **1998**, *396*, 152.

(6) Sayari, A.; Liu, P. *Microporous Mater.* **1997**, *12*, 149.

(7) Ma, Y.; Tong, W.; Zhou, H.; Suib, S. L. *Microporous Mesoporous Mater.* **2000**, *37*, 243.

(8) Braun, P. V.; Osenar, P.; Tohver, V.; Kennedy, S. B.; Stupp, S. I. *J. Am. Chem. Soc.* **1999**, *121*, 7302.

(9) Rangan, K. K.; Billinge, S. J. L.; Petkov, V.; Heising, J.; Kanatzidis, M. G. *Chem. Mater.* **1999**, *11*, 2629.

(10) MacLachlan, M. J.; Coombs, N.; Ozin, G. A. *Nature* **1999**, *397*, 681.

(11) Attard, G. S.; Bartlett, P. N.; Coleman, N. R. B.; Elliott, J. M.; Owen, J. R.; Wang, J. H. *Science* **1997**, *278*, 838.

(12) Brunel, D. *Microporous Mesoporous Mater.* **1999**, *27*, 329.

(13) Fan, H.; Lu, Y.; Stump, A.; Reed, S. T.; Baer, T.; Schunk, R.; Perez-Luna, V.; López, G.; Brinker, C. J. *Nature* **2000**, *405*, 56.

(14) Inagaki, S.; Guan, S.; Fukushima, Y.; Ohsuna, T.; Terasaki, O. *J. Am. Chem. Soc.* **1999**, *121*, 9611.

(15) Melde, B. J.; Holland, B. T.; Blanford, C. F.; Stein, A. *Chem. Mater.* **1999**, *11*, 3302.

(16) Asefa, T.; MacLachlan, M. J.; Coombs, N.; Ozin, G. A. *Nature* **1999**, *402*, 867.

(17) Yoshina-Ishii, C.; Asefa, T.; Coombs, N.; MacLachlan, M. J.; Ozin, G. A. *Chem. Commun.* **1999**, 2539.

(18) Asefa, T.; MacLachlan, M. J.; Grondley, H.; Coombs, N.; Ozin, G. A. *Angew. Chem. Int. Ed.* **2000**, *39*, 1808.

(19) Shea, K. J.; Loy, D. A.; Webster, O. W. *J. Am. Chem. Soc.* **1992**, *114*, 6700. (b) Shea, K. J.; Loy, D. A.; Webster, O. W. *Chem. Mater.* **1989**, *1*, 572. (c) Loy, D. A.; Shea, K. J. *Chem. Rev.* **1995**, *95*, 1431.

(20) Corriu, R. J. P.; Leclercq, D. *Angew. Chem., Int. Ed. Engl.* **1996**, *35*, 1420. (b) Corriu, R. J. P. *Angew. Chem., Int. Ed.* **2000**, *39*, 1376.

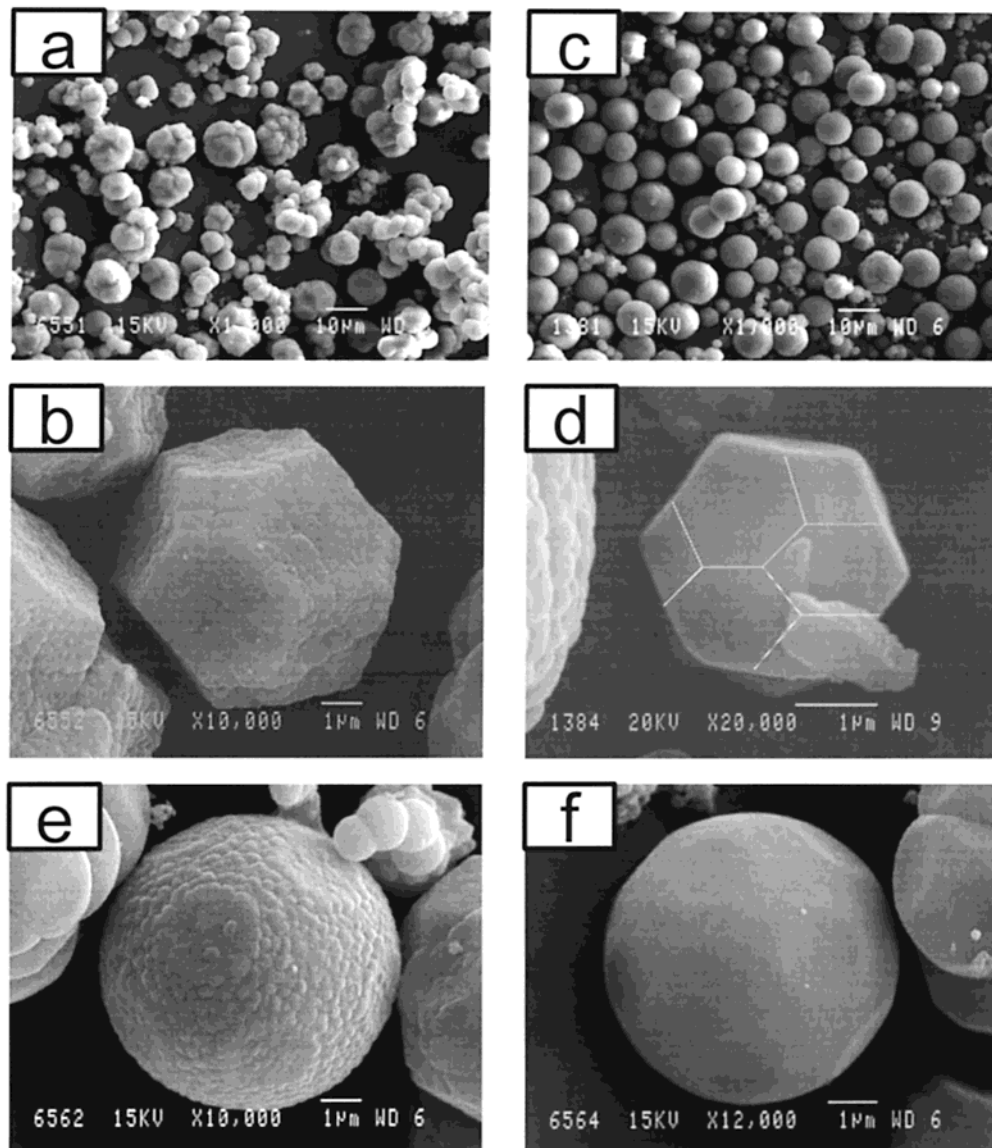


Figure 1. SEM images for the following: (a,b) $C_{16}TMACl$ -derived sample prepared using method II at 85 °C in the presence of BTME; (c–f) similar sample prepared at 100 °C. (White lines were added to (d) for clarity).

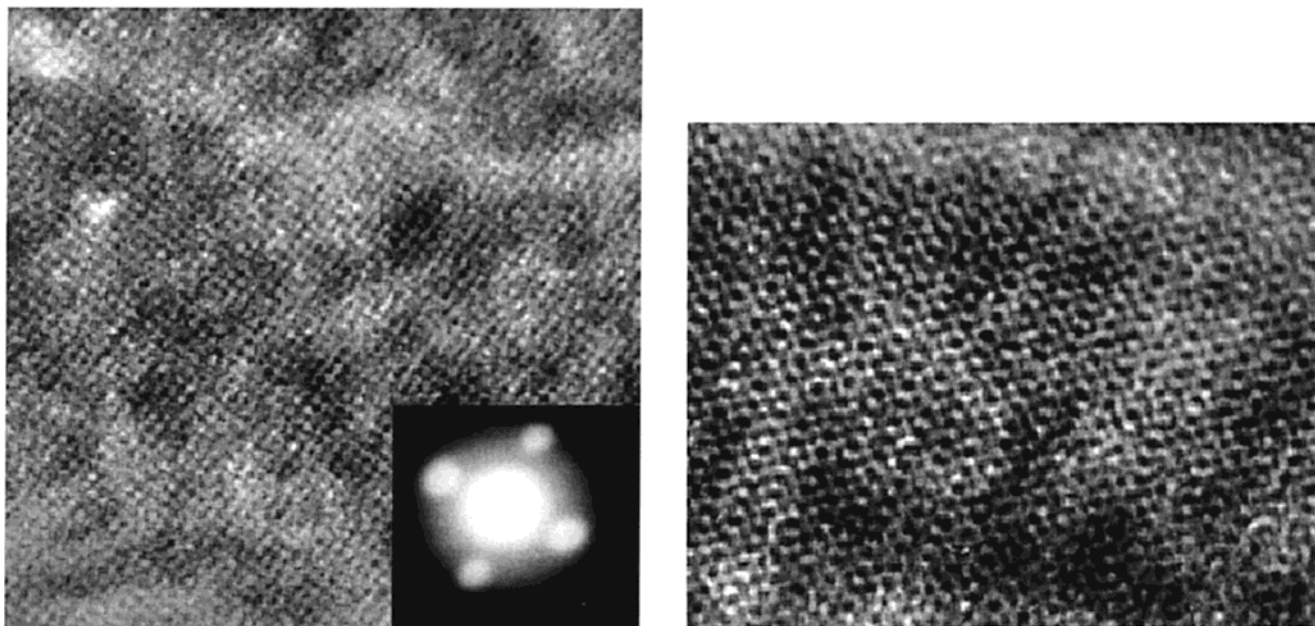


Figure 2. TEM images for the $C_{16}TMACl$ -derived sample prepared using method II at 85 °C in the presence of BTME.

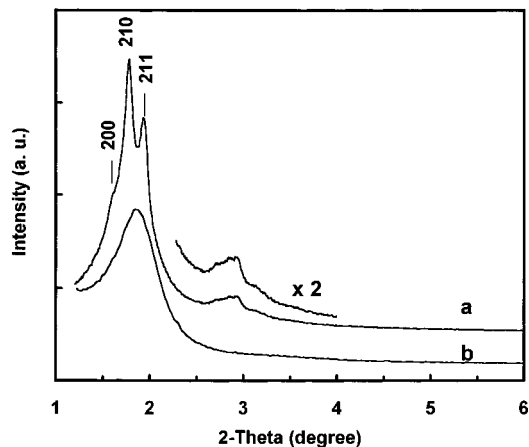


Figure 3. X-ray diffractograms for the following: (a) C_{16} -TMACl-derived sample prepared using method II at 85 °C in the presence of BTME; (b) C_{16} -TMACl-derived sample prepared using method I in the presence of BTME.

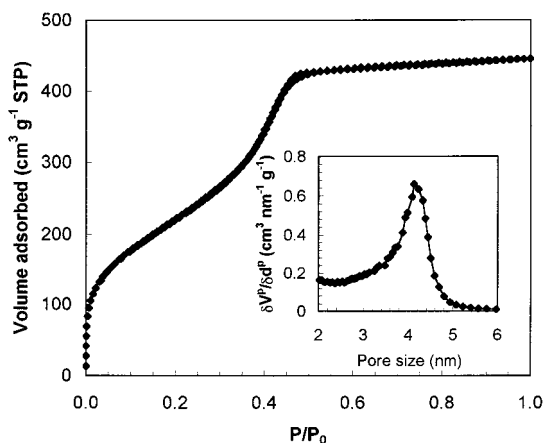


Figure 4. Nitrogen adsorption-desorption isotherm and pore size distribution for the C_{16} -TMACl-derived sample prepared using method II at 85 °C in the presence of BTME.

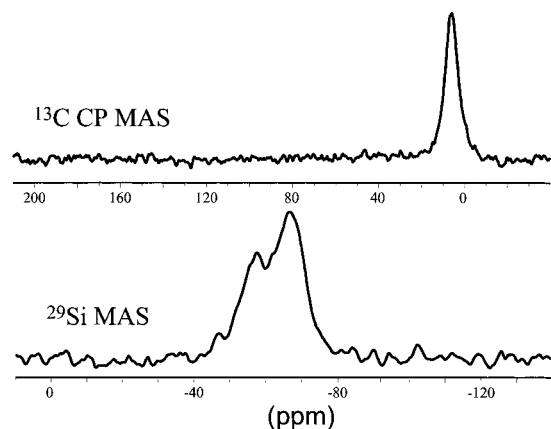


Figure 5. NMR data for the C_{16} -TMACl-derived sample prepared using method II at 85 °C in the presence of BTME.

made by Inagaki et al.¹⁴ exhibit the best resolved XRD patterns. On the basis of this observation, we adopted their preparation procedure first using cetyltrimethylammonium chloride (C_{16} -TMACl, 25% from Aldrich) as a structure-directing agent. This work was further extended to the use of octadecyltrimethylammonium chloride (C_{18} -TMACl) as first reported by Inagaki et al.¹⁴ The synthesis temperature was also varied from 85 to 100 °C.

BTME (1,2-bis(trimethoxysilyl)ethane) and BTEE (1,2-bis(triethoxysilyl)ethane) were obtained from Gelest, Inc. The surfactants C_{16} -TMACl and C_{18} -TMACl were purchased from

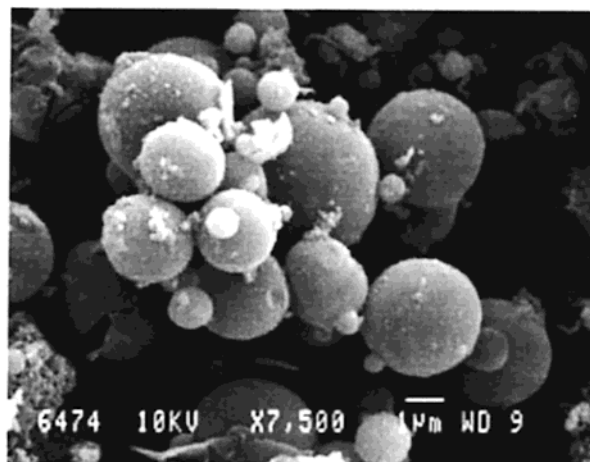
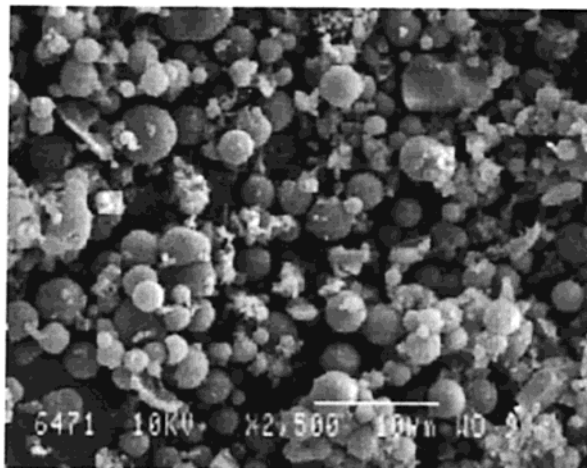


Figure 6. SEM images for the C_{16} -TMACl-derived sample prepared using method I in the presence of BTME.

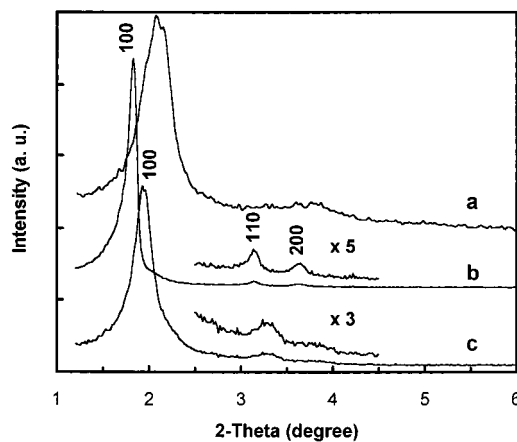


Figure 7. X-ray diffractograms for the following: (a) C_{18} -TMACl-derived sample prepared using method I in the presence of BTME; (b) C_{18} -TMACl-derived sample prepared using method II at 95 °C in the presence of BTME; (c) same sample as in (b) but using BTEE as the precursor.

Aldrich and TCI America Inc., respectively, and used without further purification. The first synthesis procedure (method I) used mixtures with the following composition: BTME (or BTEE), 1.0; C_{16} -TMACl (or C_{18} -TMACl), 0.12; NaOH, 1.0; H_2O , 231. In a typical application of this method, C_{16} -TMACl (1.54 g) was added under vigorous stirring to a solution of 0.40 g of NaOH in 40.43 g of water. After complete dissolution of the surfactant, 2.70 g of BTME was added. The stirring was continued for 24 h at room temperature while a precipitate formed. It was separated by filtration, washed thoroughly with deionized water, and dried at room temperature. The surfac-

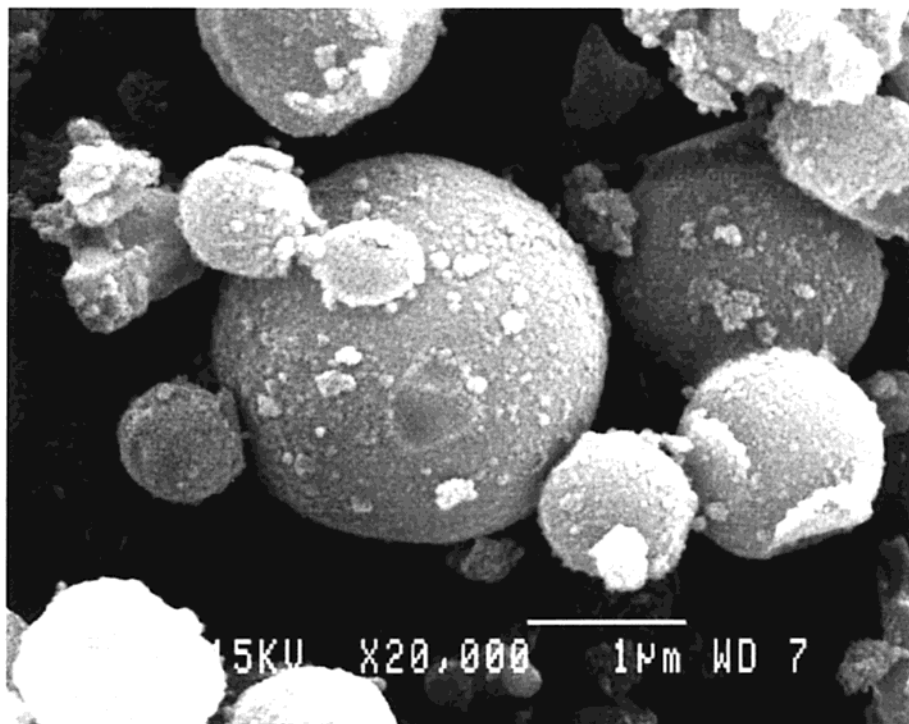


Figure 8. High-magnification SEM image for the C_{18} TMACl-derived sample prepared using method I in the presence of BTME. The surfactant was removed by solvent extraction as reported by Inagaki et al.¹⁴

The second approach (method II) used a different mixture consisting of BTME (or BTEE), 1.0; C_{16} TMACl (or C_{18} TMACl), 0.57; NaOH, 2.36; H_2O , 353. After the samples were mixed as described above, the solution was aged under stirring for 24 h at room temperature and then heated at 85–100 °C for 20–24 h without stirring. Separation of the solid and extraction of the surfactant were carried out as reported above.

Characterization. XRD spectra were obtained on a Siemens D5000 diffractometer using Cu $K\alpha$ radiation ($\lambda = 0.15418$ nm). Adsorption measurements were performed using a Coulter Ominorp 100 gas analyzer. Pore size distributions were calculated using the KJS (Kruk, Jaroniec, and Sayari) method.²¹ Scanning electron microscopy (SEM) images were recorded on a JEOL 840A microscope operated at an accelerating voltage of 10–20 kV. All SEM images reported here are representative of the corresponding materials. Transmission electron micrographs (TEM) were obtained using a Philips 430 instrument operated at 100 kV. The specimen were embedded in an epoxy resin and ultrathin sections (≈ 60 nm) were cut and examined.

^{13}C and ^{29}Si spectra were obtained at room temperature on a Bruker AMX300 instrument in a magnetic field of 7.04 T (the resonance frequencies were 75.46 and 59.6 MHz, respectively), using a 5-mm MAS probe from DOTY Scientific. The ^{13}C spectrum was recorded using cross polarization and proton decoupling. Mixing time was set to 2 ms, and 8000 scans were accumulated with a 2-s delay at a spinning speed of 4 kHz. The ^{29}Si spectrum was obtained with a simple single-pulse sequence using high-power proton decoupling. A total of 1600 scans were accumulated with a 3-min delay between the scans at a spinning speed of 8 kHz. Tetramethylsilane (TMS) was used in both cases as an external reference. Integration of the signals in the ^{29}Si spectrum was achieved by deconvoluting it into three Gaussian lines using a WINFIT simulation program from Bruker.

Results and Discussion

Cetyltrimethylammonium-Chloride-Derived Materials. Figure 1a shows a typical SEM image at low

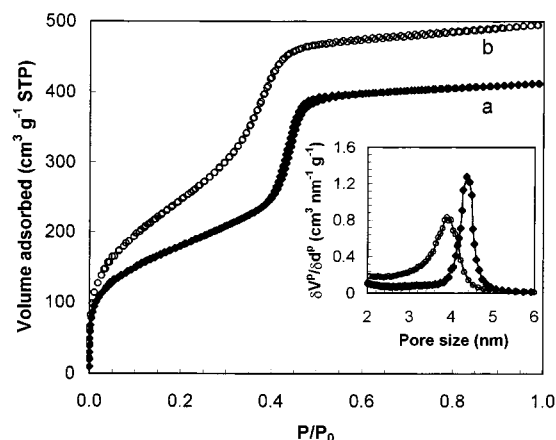


Figure 9. Nitrogen adsorption–desorption isotherm and pore size distribution for the following: (a) C_{18} TMACl-derived sample prepared using method II at 95 °C in the presence of BTME; (b) same sample as in (a) but using BTEE as the precursor.

magnification for a sample prepared according to method II at 85 °C using BTME in the presence of C_{16} TMACl. This material consisted only of isolated or agglomerated particles with truncated rhombic dodecahedral particles (Figure 1b) reminiscent of those observed recently for MCM-48 silica.^{22,23} Most particles exhibited quite rough surfaces. The particle shape is consistent with a cubic structure. This conclusion is also supported by TEM measurements (Figure 2). At first glance, samples prepared at slightly higher temperature (95–100 °C) appear to be comprised mainly of ≈ 10 - μm spheres (Figure 1c) with the same rough surfaces as the faceted particle shown in Figure 1b. However, close inspection of such spheres shows that they exhibit a number of circular flat areas, all linked to each other via the

(21) Kruk, M.; Jaroniec, M.; Sayari, A. *Langmuir* **1997**, *13*, 6267.

(22) Kim, J. M.; Kim, S. K.; Ryoo, R. *Chem. Commun.* **1998**, 259.

(23) Sayari, A. *J. Am. Chem. Soc.* **2000**, *122*, 6504.

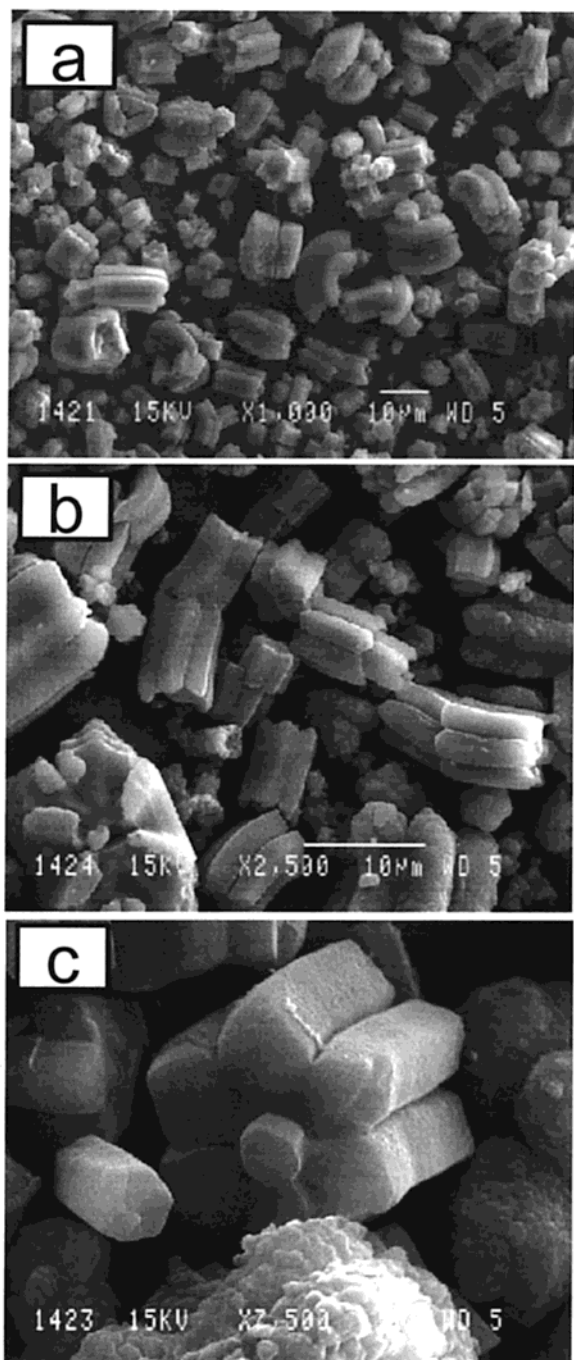


Figure 10. SEM images for the C_{18} TMACl-derived sample prepared using method II at 100 °C in the presence of BTME. symmetry operations that exist between the hexagonal faces of the truncated rhombic dodecahedra. For example, Figure 1e shows a spherical particle with four flat circular areas remnant of the four hexagonal faces in Figure 1b, which are images of each other through the 4-fold symmetry operation. In addition, samples prepared at 95–100 °C (Figure 1c) also exhibit a limited number of particles such as those shown in Figure 1d,f. These particles are respectively similar to those shown in Figure 1b,e, the main difference being their smooth surface. It is interesting to notice that in addition to the four flat circular areas, the particle in Figure 1f exhibits along its edges an additional four flat areas that correspond to what remains from the original square faces. This indicates clearly that the truncated rhombic dodecahedra grow gradually into spherical particles.

Scheme 1

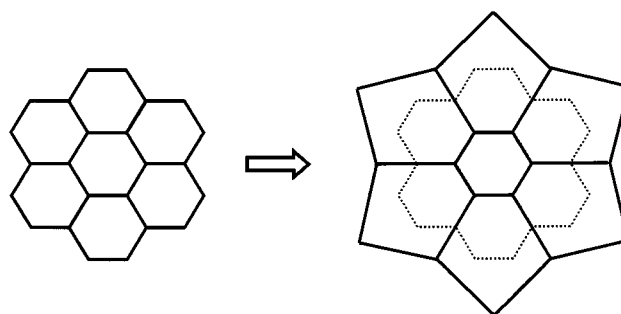


Figure 3a shows a typical XRD spectrum for a cubic sample prepared at 85 °C. We were able to fit the first three main peaks to the (200), (210), and (211) diffraction lines for a P-type cubic structure with a unit cell $a = 11.02$ nm. Owing to the strong similarity between this diffractogram and that of SBA-1 ($Pm3n$) silica,²⁴ it is inferred that our material belongs to the same space group. Figure 4 shows the corresponding N_2 adsorption–desorption isotherm and the pore size distribution. The surface area for cubic materials made in the presence of C_{16} TMACl was in the range 650–850 $m^2 g^{-1}$, whereas the pore size and volume were ≈ 3.8 –4.0 nm and 0.7 $cm^3 g^{-1}$, respectively.

^{13}C CP MAS NMR (Figure 5) data showed that, after extraction, these materials exhibit one single peak at 5.9 ppm, which is unambiguously attributable to methylene groups covalently linked to Si. The ^{29}Si MAS NMR spectrum exhibited three peaks at -66.5 , -57.5 , and -47.0 , whose relative intensities were in order 60, 36, and 4%. The first peak was attributed to fully condensed silicon $CSi(OSi)_3$. The two other peaks were assigned to partially hydrolyzed Si species, that is, $C(OH)Si(OSi)_2$ at -57.5 ppm and $C(OH)_2Si(OSi)$ at -47.0 ppm. It is important to notice that all silicon atoms were covalently connected to a carbon atom.

Using method I in the presence of C_{16} TMACl afforded materials comprised of spherical particles with rough surfaces and a relatively wide distribution of sizes from ≈ 0.5 to 5 μm (Figure 6). This indicates that contrary to the materials described above, the spherically shaped particles in the current organosilica occurred since the beginning of the growth process. Moreover, as will be shown later (see Figure 8), these spheres are not single particles. They actually result from the agglomeration of much smaller particles. The N_2 adsorption isotherm exhibited the now well-known characteristic features for periodic mesoporous materials with narrow pore size distributions. The pore size, pore volume, and the BET surface area were in order 2.9 nm, 0.7 $cm^3 g^{-1}$, and 1150 $m^2 g^{-1}$. As for the XRD pattern (Figure 3b), it consisted of mainly a single broad peak. Using method I in the presence of C_{18} TMACl, Inagaki et al.¹⁴ synthesized three-dimensional hexagonal mesoporous organosilica. Similar to the current material, Inagaki et al.'s material consisted also of 0.1–10- μm spheres with high surface area (1170 $m^2 g^{-1}$). It is thus suggested that despite the fact that our XRD pattern is not well resolved, the C_{16} -TMACl-derived material via the synthesis method I has also three-dimensional hexagonal symmetry.

(24) Huo, Q.; Margolese, D. I.; Ciesla, U.; Demuth, D. G.; Feng, P.; Gier, T. E.; Sieger, P.; Firouzi, A.; Chmelka, B. F.; Schüth, F.; Stucky, G. *Chem. Mater.* **1994**, *6*, 1176.

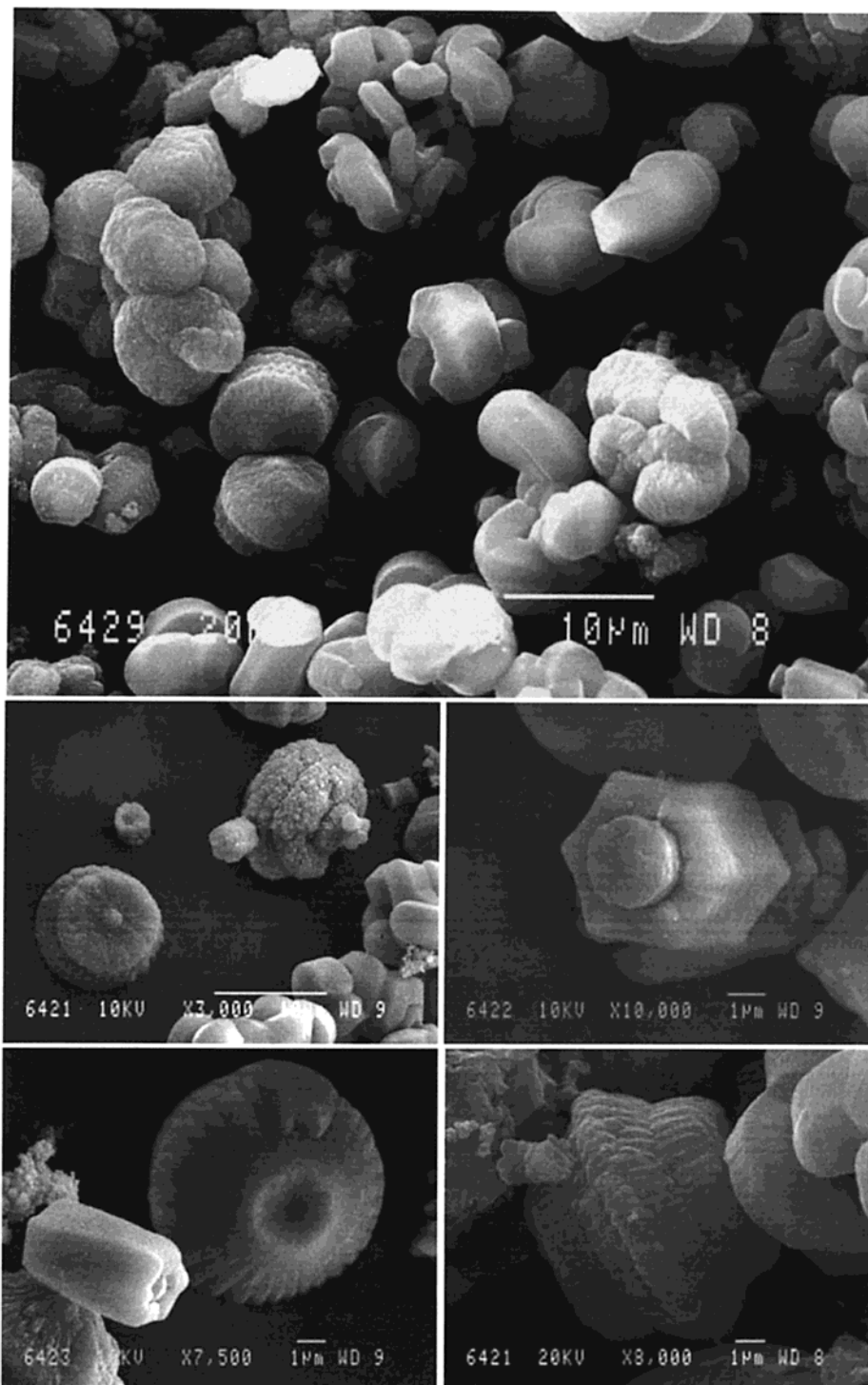


Figure 11. SEM images for the C_{18} TMACl-derived sample prepared using method II at 95 °C in the presence of BTME.

Octadecyltrimethylammonium-Chloride-Derived Materials. In agreement with Inagaki et al.,¹⁴ using method I in the presence of BTME as a precursor led to a periodic mesoporous organosilica with three-dimensional hexagonal structure. This material exhibited similar morphology, XRD pattern (compare Figures 7a and 3b), and structural properties as its C_{16} TMACl-derived counterpart (see Figure 6). The pore size, pore volume, and the BET surface area were in order 3.3 nm, $0.76 \text{ cm}^3 \text{ g}^{-1}$, and $1202 \text{ m}^2 \text{ g}^{-1}$. As alluded to earlier, Figure 8 clearly shows that the spherical particles,

regardless of their size, do not seem to be single particles, but are rather comprised of much tinier ($<0.1 \mu\text{m}$) particles.

As indicated by the narrow and well-resolved XRD peaks (Figure 7b), by the sharp nitrogen condensation step (Figure 9a), and by the narrow pore size distribution, method II using BTME afforded excellent quality materials in terms of framework periodicity. All materials exhibited two-dimensional hexagonal structure similar to that of MCM-41 silica, with $d_{100} = \approx 4.85$ - and 4.4-nm pores. This results in a pore wall thickness of $\approx 1.2 \text{ nm}$, similar to that of typical MCM-41 silicas.^{21,25} In addition, these samples exhibited some unique mor-

(25) Kruk, M.; Jaroniec, M.; Sayari, A. *J. Phys. Chem. B* **1997**, *101*, 583

phologies strongly dependent on synthesis temperature. One sample made at 100 °C was almost entirely comprised of $\approx 10\text{-}\mu\text{m}$ faceted rods (Figure 10a) concentrically self-assembled in sets of six rods (Figure 10b). The central part of this assemblage was often empty, but sometimes, as shown in Figure 10c, it was occupied by a single rod. Also, as shown in Figure 10b, a second layer of rods may self-assemble around the first one. Close inspection of Figure 10c (and other particles in Figure 10b) shows that the outermost facets of the tubules are at a lower than 120° angle to each other. In this case, they were actually almost perpendicular, which seems to be noncompatible with the hexagonal symmetry of the material. As shown in Scheme 1, this is most likely due to the fact that at the time the tubules self-assembled, they exhibited hexagonal sections, but the growth process continued. The faster, outward growth compared to very slow, or most likely absence of, growth for the inner facet led to more and more deformation of the hexagonal section of the tubules. Ultimately, as shown in Figure 10c, only five faces persisted, the inner one being the smallest and the outermost facets may be perpendicular to each other.

Another sample prepared using method II in the presence of BTME at a slightly lower temperature gave rise to a material with a very well ordered two-dimensional hexagonal structure and very rich morphological features. This sample had $656\text{ m}^2\text{ g}^{-1}$ surface area, $0.64\text{ cm}^3\text{ g}^{-1}$ pore volume, and 4.2-nm pores. Figure 11 shows that, in addition to the ubiquitous faceted tubules, this sample contained particles with exotic shapes akin to those obtained in the $\text{C}_{16}\text{TMACI}$ -tetraethyl orthosilicate system under quiescent aqueous acidic conditions,²⁶ and also in tetramethyl orthosilicate block copolymer,²⁷ or aluminum nitrate-sodium dodecyl sulfate-urea²⁸ systems.

Similar to BTME, using method I in the presence of BTEE gave organosilica with a three-dimensional hexagonal structure, but the particles did not exhibit any particular shape. The pore size, pore volume, and the BET surface area for this material were in order 3.1 nm , $0.57\text{ cm}^3\text{ g}^{-1}$, and $1029\text{ m}^2\text{ g}^{-1}$. Interestingly, method II at 95°C afforded excellent quality material with a two-dimensional hexagonal structure. The corresponding XRD pattern is displayed in Figure 7c, whereas the N_2 adsorption-desorption isotherm and pore size distribution are shown in Figure 9b. This sample exhibited $904\text{ m}^2\text{ g}^{-1}$ surface area, $0.77\text{ cm}^3\text{ g}^{-1}$ pore volume, and 3.9-nm pores. It was comprised mainly of unusually long hexagonally faceted particles up to $30\text{--}40\text{ }\mu\text{m}$ in length (Figure 12, upper frame). Moreover, in contrast to all particles with similar shapes reported in the literature, close-up images of the current tubules (Figure 12, lower frame) indicate that their central part is empty.

Conclusion

High-quality periodic mesoporous organosilicas were prepared using bridged silsesquioxane species as precursors via the so-called supramolecular templating

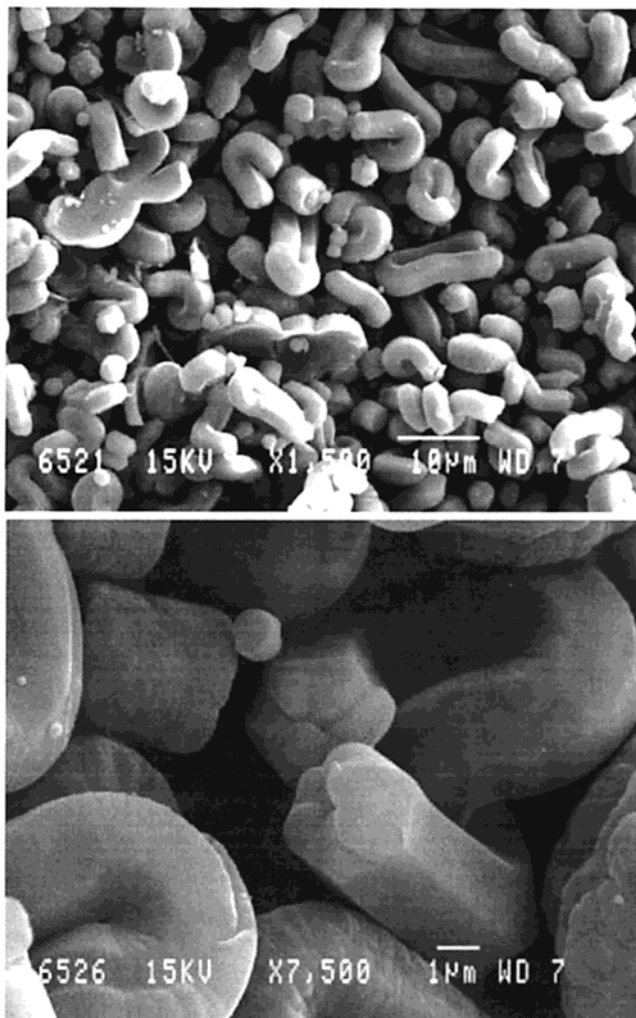


Figure 12. SEM images for the $\text{C}_{18}\text{TMACI}$ -derived sample prepared using method II at 95°C in the presence of BTEE. approach known to afford M41S and related silica mesophases. Both two-dimensional and most likely three-dimensional hexagonal as well as cubic ($Pm3n$) structures were obtained. In some cases, SEM observations provided unique insights into the growth process of such materials. For example, in the case of organosilica with cubic structure, spherical particles grew out of truncated rhombic dodecahedra. Some preparations led to materials comprised of particles with unique morphologies.

Acknowledgment. While this manuscript was almost completed, Dr. Inagaki²⁹ described in a recent meeting a cubic organosilica with similar faceted particles as the material described here, but prepared using a higher $\text{C}_{16}\text{TMACI}/\text{BTME}$ ratio (0.91 vs 057). He also referred to a paper in Web format.³⁰ Similarly, Dr. Brinker³¹ mentioned in the same meeting that he made recently porous organosilica films and particulates using bridged silsesquioxane monomers.

CM000479U

(29) Inagaki, S.; Guan, S.; Fukushima, T.; Ohsuna, T.; Terasaki, O. Presented at Access in Nanoporous Materials II, Banff, Alberta, Canada, May 26–28, 2000.

(30) Guan, S.; Inagaki, S.; Ohsuna, T.; Terasaki, O. *J. Am. Chem. Soc.* **2000**, *122*, 5660.

(31) Lu, Y.; Fan, H.; Doke, N.; Loy, D. A.; Assink, R. A.; LaVan, D. A.; Brinker, C. J. *J. Am. Chem. Soc.* **2000**, *122*, 5258.

(26) Yang, H.; Coombs, N.; Ozin, G. A. *Nature* **1997**, *386*, 692.

(27) Zhao, D.; Sun, J.; Li, Q.; Stucky, G. D. *Chem. Mater.* **2000**, *12*, 275.

(28) Yada, M.; Hiyoshi, H.; Ohe, K.; Machida, M.; Kijima, T. *Inorg. Chem.* **1997**, *36*, 5565.